Received: 7 April 2023 | Revised: 15 May 2023 | Accepted: 19 May 2023 | Published online: 24 May 2023

RESEARCH ARTICLE

Journal of Computational and Cognitive Engineering
2024, Vol. 00(00) 1–11
DOI: 10.47852/bonviewJCCE3202943

BON VIEW PUBLISHING

Improved PCNN Polarization Image Denoising Method Based on Grey Wolf Algorithm and Non-Subsampled Contourlet Transform

Yuhai Li[1], Yuxin Sun[1,*] and Kai Feng[1]

[1]*Science and Technology on Electro-Optical Information Security Control Laboratory, China*

Abstract: In this article, an adaptive pulse-coupled neural network (PCNN) polarization image denoising method based on Grey Wolf Optimization (GWO) and Non-subsampled Contourlet Transform (NSCT) is proposed. Different from the traditional PCNN denoising method, the captured polarization image was firstly devised by the NSCT and enforced band-decomposition to denoised by PCNN. The evaluable index of the image was used for quantitative analysis. Then, GWO is used to update PCNN inherent voltage constant and attenuation time constant and neurons connected intensity factor three model parameters, after looking for multiple optimal solutions, and then to polarized image denoising to achieve the best effect. This method not only avoids the image edge blurring caused by the traditional image denoising method, but also solves the problem that the parameters of the PCNN are difficult to accurately estimate. Hence, it is more suitable for polarization images containing noise. The experiment and the quantitative analysis of image evaluation indices showed that NSCT-GWO-PCNN effectively suppresses the noise in polarization image by reducing salt-and-pepper noise while protecting edges.

Keywords: polarization image, Grey Wolf Optimization, Non-subsampled Contourlet Transform, image denoising, pulse-coupled neural network

1. Introduction

In recent years, polarized light has been widely used to obtain multi-dimensional information about objects in the fields of object detection and sensing. Most polarization images must be processed and transmitted to provide useful information about the target, expand the detection range, and perform polarization light navigation based on the relations among polarization channels. However, in the process of obtaining a polarization image, because of the uneven distribution of the polarization camera micro-polarization array and high levels of noise in weak sunlight, the quality of the polarization image will be severely reduced, and polarization information is extremely difficult to extract [1]. Therefore, to improve the discriminability of polarization images, effective denoising needs to be performed.

The pulse-coupled neural network (PCNN) is an effective nonlinear digital data analysis method that consists of complex models of the input and feedback systems. It has the functional features of synchronous firing of neurons in multiple states and synchronous spike release. It can search for and isolate noise points according to the firing patterns of different neurons. High-intensity noise points are eliminated by nonlinear transformation and modulation, and hence this method has been applied in image denoising. Lindblad and Kinser [2] modified the PCNN firing model and changed the cyclic firing to one firing event to locate impulse noise using a PCNN; Shi et al. [3] further adapted the method for image filtering by improving the hard-limiting function of the PCNN; Li et al. [4] proposed an improved PCNN and Otsu-based image enhancement method, which increases the signal-to-noise ratio (SNR) after image filtering; Fang et al. [5] reduced the time complexity of PCNNs by simplifying the model, threshold lookup table, and overall calculations in a specific implementation of a PCNN; Guo et al. [6] conducted in-depth research on the use of PCNNs for binary image denoising and image smoothing and proposed an image denoising algorithm based on PCNN; and Wang et al. [7] used the parallel computing power of quantum computing to solve the problem of large computation amount in neural network. Based on the PCNN, the authors propose the quantum PCNN.

Few works exist on denoising algorithms for polarization images. Gilboa et al. [8] proposed an interpolation algorithm based on the Gaussian regression process to denoise polarization images. The algorithm also verifies that the accuracy of the denoised polarization image will be affected if noise is not considered. Zhang et al. [9] proposed a denoising algorithm for polarization images based on principal component analysis (PCA). The algorithm exploits the fact that the four polarization channels of an ideal noise-free polarization image are correlated, while the noise is random and uncorrelated. The covariance matrix between the two polarization channels is projected onto the PCA domain, and poor correlation among the four polarization channels is eliminated as noise using the dimensionality reduction characteristics of PCA. Deng et al. [10] proposed a new working

*Corresponding author: Yuxin Sun, Science and Technology on Electro-Optical Information Security Control Laboratory, China. Email: sunyuxin114855@163.com

mode for the PCNN, where the refiring of fire-extinguishing neurons is only allowed when all firing neurons are extinguished. They also work out the constraint conditions of the parameter settings under this mode. The polarization image denoising methods often cause blurring at the images of different polarization channels, and it is difficult to estimate the parameters of the denoising model using the PCNN algorithms.

Many important parameters need to be precisely set when PCNN is used for image denoising, but these parameters can only be estimated manually through the amount of experiments, which requires not only a large workload but also low model accuracy. Non-subsampled Contourlet Transform (NSCT) can achieve multi-bands decomposition of effective information separation in polarization images. Grey wolf optimization (GWO) is used to optimize the fitness function of PCNN to improve the model search efficiency and generalization ability, which finally solves the above problems.

In summary, this article proposes an adaptive PCNN polarized image denoising method based on GWO and NSCT. Firstly, polarization image decomposed by NSCT. Then, after successive hierarchical screening and multiple iterations of GWO, the parameters of the PCNN are optimized globally accurately, which not only effectively solves the problem of setting the key parameters of the PCNN but also greatly improves the computational speed of the whole model. The optimized PCNN with GWO is used to denoise different parameters, which finally eliminated the high-intensity noise and makes the whole denoising process more effective. The results show that the proposed polarization image denoising method not only extracts and preserves the image details but also effectively suppresses the noise.

2. NSCT-GWO-PCNN-Related Work

2.1. PCNN biologically inspired model

The PCNN is an effective nonlinear digital data analysis method that consists of complex models of the input and feedback systems. It has the functions of neuron-specific linear addition, biological electrical pulse transmission, nonlinear modulation, synchronous pulse release, and so on [11]. Unlike other neural networks, PCNN can extract and isolate image pixel information without learning or training parameters. The PCNN model consists mainly of a branching tree system input, an operation linker, and a pulse generator, as shown in Figure 1.

When a PCNN is used for data image processing, a two-dimensional polarization image corresponds to a two-dimensional PCNN neural network of the same size. The gray value of the pixel corresponds to the initial external stimulus of the neuron at the corresponding position [12, 13]. The gray value is used as the dynamic input for each neuron and a dynamic threshold is set. If the input gray value is greater than the neuron's dynamic threshold, the neuron is activated, that is, the neuron whose internal activation is higher than the dynamic threshold enters the firing state. Because the individual neurons of a PCNN are connected to other neurons, the state of a single neuron affects the states of the surrounding neurons. If a single neuron fires, an external excitation is fed to the neighboring neurons. If the neighboring neurons are not firing and their internal activation is above than the dynamical threshold after external excitation, they will be in the activated firing state as a single neuron.

Figure 1
PCNN model

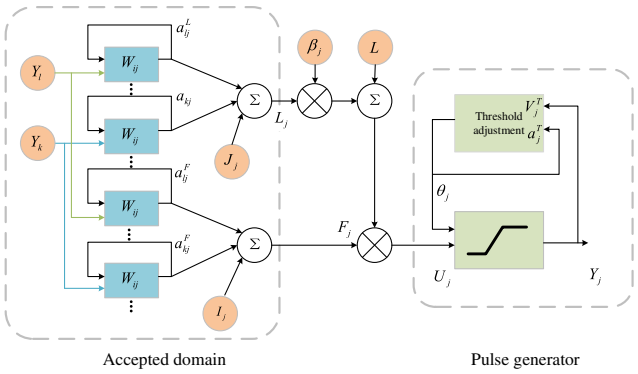

To meet the needs of image denoising, a simplified PCNN neuron model without leaky integrators in the input and connection domains is used. There are three parameters to determine: the inherent voltage constant V_T, attenuation time constant α_T, and neuron connection intensity factor β_T. The algorithm of the simplified PCNN model is roughly as follows: First, input a grayscale image to the PCNN model as follows [14]:

$$F_{ij}[n] = I_{ij} \tag{1}$$

where F_{ij} represents the input signal of the PCNN model. Here, image I_{ij} is used as the input signal of the PCNN model, that is, point (i, j) corresponds to the grayscale value of the image pixel. After the noisy signal has been input, the internal activity term U_{ij} is calculated as follows:

$$L_{ij}[n] = \sum_{B} W_{iji} Y_k[n-1] \tag{2}$$

$$U_{ij}[n] = F_{ij}[n]\{1 + \beta_T L_{ij}[n]\} \tag{3}$$

Then, internal activation U_{ij} is compared with neuron dynamic threshold E_{ij} to generate a pulse output Y_{ij} as follows:

$$Y_{ij}[n] = \begin{cases} 1, & U_{ij}[n] > E[n-1] \\ 0, & U_{ij}[n] > E[n-1] \end{cases} \tag{4}$$

When the state of $Y_{ij}[n]$ is 1, the neuron is activated and outputs a high value; when the state is 0, the neuron is in a dormant state and outputs a low value.

When PCNN models are used for image denoising, several neurons with a feedback structure are used for the firing operations. The number of neurons is determined by the number of pixels of the image, that is, the number of neurons in the PCNN network is equal to the number of pixels in the input polarization image. In the PCNN model, it is necessary to exploit the influence of the peripheral neuron state on the central neuron state and convert it into the signal intensity transmitted to the central neuron, which is expressed by a weighted coefficient matrix, defined as follows:

$$W_{ijkl} = \frac{1}{\sqrt{(i-k)^2 + (k-l)^2}} \tag{5}$$

where (i, j) and (k, l) are the coordinates of the grayscale pixels of the polarization image. The relationship between the complete PCNN image denoising model and image pixels is illustrated in Figure 2.

Figure 2
Relationship between image pixels and the PCNN

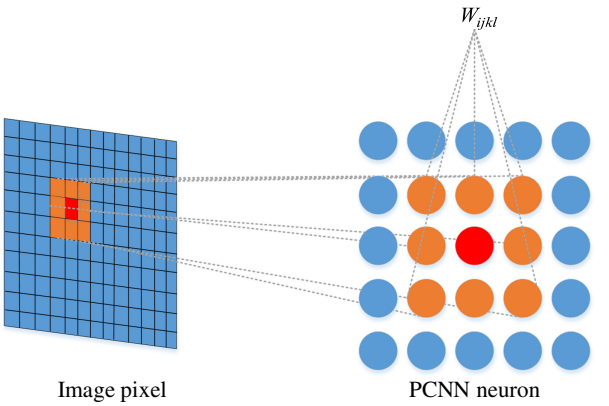

2.2. Non-Subsampled Contourlet Transform

The NSCT is a multi-scale geometric transformation. It can provide information in any direction of the polarization image, because it contains non-subsampling pyramid filter bank and non-subsampling directional filter bank. The NSCT divides the polarization image into many sub-bands. Background and untextured areas of the polarization image belong to low-pass sub-bands, and the edge details and noises belong to high-pass sub-bands.

The ideal passband support of the low-pass filter at the j-th stage is the region $[-(\pi/2^j),(\pi/2^j)]^2$ in NSCT. Accordingly, the ideal support of the equivalent high-pass filter is the opposite region of the low-pass: $[-(\pi/2^{j-1}),(\pi/2^{j-1})]^2\backslash[-(\pi/2^j),(\pi/2^j)]^2$ [15]. The j-level equivalent filter that decomposes images can be expressed by the following equation:

$$H(z)=\begin{cases} H_1(z)\prod_{j=0}^{J-2}H_0(z^{2j}), 1\le j\le 2^J \\ \prod_{j=0}^{J-2}H_0(z^{2j}), j=2^J \end{cases} \tag{6}$$

Multi-scale analysis of polarization image can be performed by convolving the equivalent filter [16]. The j-level decomposition of polarization image in the k-th can produce a low-pass sub-bands images and $\sum_{j=1}^{J}2^{l_j}$ band-pass sub-bands images (l_j represents the direction decomposition at the j-level), and corresponding coefficients can be expressed as

$$\left\{c_{j_0}(m,n),c_{j,l}(m,n)(j_0\ge j\ge 1,l=1,2,\ldots,2^{l_j})\right\}_k \tag{7}$$

where $c_{j0}(m,n)$ denotes low-pass sub-bands coefficients at the j_0-th scale; $c_{j,l}(m,n)$ denotes band-pass sub-bands coefficients at the j-th scale and the l-th direction. Figure 3 shows the effect of NSCT band decomposition. The purpose of this method is to adopt different denoising strategies for images with different frequency sub-bands to avoid the loss of important image details in the process of denoising. Since most of the noise belong to the high-frequency bands, radical denoising strategy is adopted for it, while the low-frequency band is not processed or treated lightly.

2.3. GWO optimization algorithm

Heuristic optimization algorithms that have been inspired by related physical phenomena, animal behaviors, have been widely used in many scientific fields. GWO is a heuristic technique [17]

Figure 3
NSCT band decomposition for polarization image

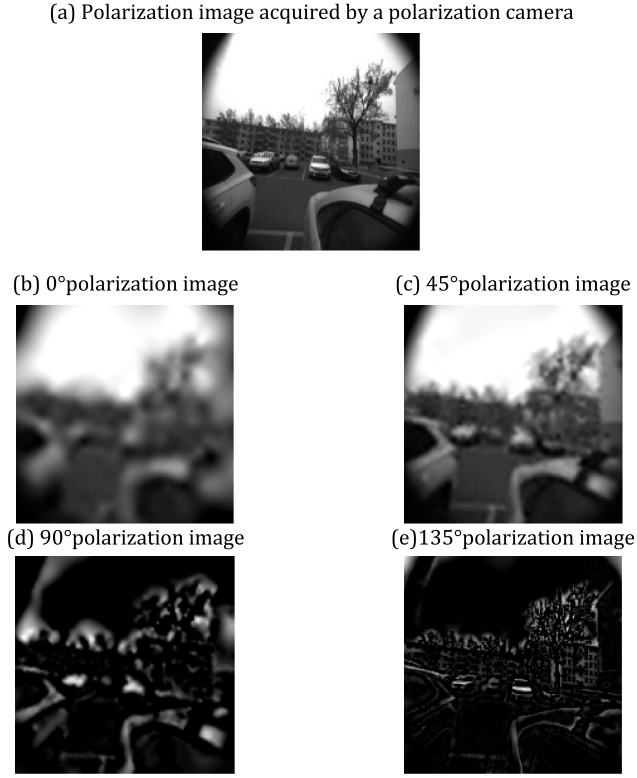

based on the behaviors of wolf packs proposed by Mirjalili et al. [18]. GWO is inspired by the strategy wolves used to catch prey. Since GWO can solve optimization functions, it can be further applied to complex multivariate solving problems. For example, PCNN contains a model with multiple parameters that must be optimized. The initial phase of GWO in the search process is prey encirclement. The formula for simulating the encircling process is as follows [19, 20]:

$$\vec{D}=\left|\vec{C}\cdot\vec{X}_P(t)-\vec{X}(t)\right| \tag{8}$$

$$\vec{X}(t+1)=\vec{X}_P(t)-\vec{A}\cdot\vec{D} \tag{9}$$

where t represents the current iteration, and $\vec{X}_P$, $\vec{X}$ are the position vectors of the prey and gray wolves, respectively. Vectors $\vec{A}$ and $\vec{C}$ are calculated as follows:

$$\vec{A}=2\vec{a}\cdot\vec{r}_1-\vec{a} \tag{10}$$

$$\vec{C}=2\cdot\vec{r}_2 \tag{11}$$

where $\vec{r}_1$ and $\vec{r}_2$ are random vectors in [0,1]. Using these vectors, the position can be updated randomly on the search domain; $\vec{a}$ is a motion vector that decreases linearly during the iteration.

The wolf pack consists of four types of wolves: α, β, δ, and ω. We assume that α, β, and δ know more about the location of the prey. Therefore, the ω wolves must update their positions according to the three best positions obtained so far [21]. The characteristics of the wolves can be expressed numerically as

$$\begin{cases} \vec{D}_\alpha = \left|\vec{C}_1 \cdot \vec{X}_\alpha - \vec{X}\right| \\ \vec{D}_\beta = \left|\vec{C}_2 \cdot \vec{X}_\beta - \vec{X}\right| \\ \vec{D}_\delta = \left|\vec{C}_3 \cdot \vec{X}_\delta - \vec{X}\right| \end{cases} \tag{12}$$

$$\begin{cases} \vec{X}_1 = \left|\vec{X}_\alpha - \vec{A}_1 \cdot \vec{D}_\alpha\right| \\ \vec{X}_2 = \left|\vec{X}_\beta - \vec{A}_2 \cdot \vec{D}_\beta\right| \\ \vec{X}_3 = \left|\vec{X}_\delta - \vec{A}_3 \cdot \vec{D}_\delta\right| \end{cases} \tag{13}$$

$$\vec{X}(t+1) = \frac{\vec{X}_1 + \vec{X}_2 + \vec{X}_3}{3} \tag{14}$$

The initial solutions α, β, and δ are obtained individually, and the rest of the solutions cancel out simultaneously. The average value of the three optimal solutions is expressed as $\vec{X}$. After the prey is attacked and stops moving, the hunt process will stop. Then the above cycle repeats. If $\overrightarrow{A} < 1$, the attack process ends; otherwise, if $\overrightarrow{A} >; 1$, the gray wolf shifts its attention and begins to search for prey again.

3. NSCT-GWO-PCNN Polarization Image Denoising Method

Polarization imaging is an emerging optical imaging technique. In contrast to the arrays used for intensity imaging, the polarization array of current optical polarization imaging devices has four polarization angles: 0°, 45°, 90°, and 135°. A camera equipped with this polarization array can collect four polarization images with different illumination intensities according to the polarization information of sunlight. A variety of target information can be obtained for detection and navigation from the polarization characteristics of sunlight in the obtained polarization image. Figure 4 shows a polarization image of a scene on a sunny day taken by a polarization camera. Polarization images with different intensities due to different polarization angles after decomposition are also shown.

In the polarization images in Figure 3, there are particle noise points in the light intensities under different polarization angles. Therefore, the NSCT-GWO-PCNN denoising method proposed in this article is used for noise removal. In contrast to denoising conventional images, when processing polarization images, we denoise the four polarization angle images separately and finally merge the four images into a complete polarization image.

The flow chart of the proposed method based on NSCT-GWO-PCNN is shown in Figure 5.

To combine the evaluation of the PCNN image denoising with the GWO goal, the fitness function [22] is that each set of optimization parameters must meet the requirements of the objective function, and the parameter set with the largest fitness value is obtained after screening, as follows:

$$h = 10^* \log\left(\frac{255^2}{\theta}\right) \tag{15}$$

$$\theta = 10^* \log\left(\frac{\left\|S - Y\right\|_P^2}{M \cdot N}\right) \tag{16}$$

where h is the fitness criterion, θ is the mean squared error (MSE), S is the original input image, $\|S - Y\|$ is the $p(p = 2)$ norm of $S - Y$, and M and N denote the dimensions of the original and denoised images. The steps of the GWO-PCNN are listed in Algorithm 1.

Figure 4
Original polarization image and the decomposed images of each polarized light channel

(a) Polarization image acquired by a polarization camera

(b) 0°polarization image

(c) 45°polarization image

(d) 90°polarization image

(e)135°polarization image

2

Algorithm 1. NSCT-GWO-PCNN image denoising algorithm

Algorithm: NSCT-GWO-PCNN image denoising algorithm

Step 1: Border processing

Generate an edge symmetrical expansion so that the input image (m, n) is expanded to $(m + 6, n + 6)$;

Step 2: NSCT

Compute NSCT band coefficients $c_{j,l}(m, n)$

Step 3: GWO optimization of the PCNN parameters α_T, β_T, V_T

Initialize the number of wolves (i=1, 2, …, N) and maximum number of iterations N, a, A, C; Set the PCNN parameters α, β, δ wolves respectively, and solve the function fitness value h of every group of parameters;

Maintain each pixel in a non-firing state;

If $t < N$, end after updating the location of the current search agent, update, A, and C;

Solve the function fitness value of all search agents h;

$t = t$+1;

Update the first search agent Y_a, the second search agent Y_β, and the third search agent Y_V;

End when $t < N$, otherwise continue to search for the three best agents;

Step 4: Noise detection and processing

Calculate the value of $L_{ij}[n]$ for each neuron in the 3 × 3 regions;

Adjust the threshold of $L_{ij}[n]$;

Calculate the value of the $L_{ij}[n]$ modulation signal inside the neuron;

Figure 5
GWO-PCNN image processing

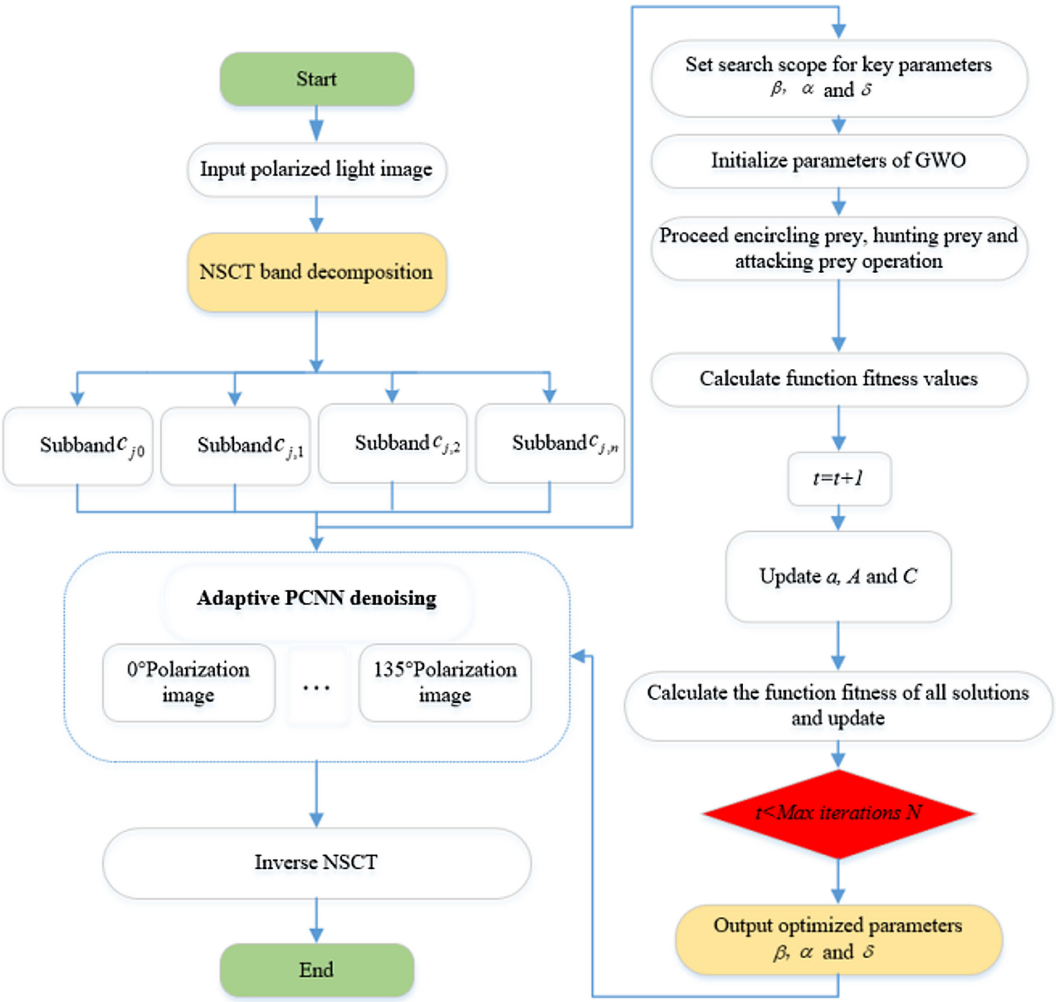

If one neuron in the adjacent area is fired, and more than four adjacent neurons are not fired at the same time, the brightness $U_{ij}[n]$ of the pixel will decrease at the end of the step Δt;

Otherwise, the brightness value of the image pixel does not change;

Step 5: Compare the values of and $E_{ij}[n]$

Step 6: Record the output

Record the output state of neurons: activated or inactivated;

Step 7: Determine whether to loop

$N = N - 1$, and $N \neq 0$, loop step 3;

otherwise, end the program.

4. Experiment and Analysis

4.1. Convergence and adaptation analysis

In order to verify the effectiveness of GWO improvement strategy, four kinds of international benchmark test functions are selected for simulation and comparison experiments. In order to ensure unbias, the population number N of GWO is set as 30, and the total number of iterations is set as 500. In order to eliminate the influence of randomness, all experiments were run independently for 4 times, and the mean value and STD (standard deviation) of the 4 times were taken as the measurement standard of algorithm performance.

The mathematical formula of the test functions is shown in Table 1, including two single-peak test functions (F1, F2) and two multi-peak test functions (F3, F4). The single-peak test function is a measure of the algorithm's solving accuracy and convergence speed, while the multi-peak test function can well represent the algorithm's global searching ability and the ability to avoid local optimization. Figure 6 shows the two-dimensional search space of partial single-peak and multi-peak test functions.

In order to prove the advantages of GWO convergence, three classic, mainstream approaches, Genetic Algorithm (GA) [23], Ant Colony Algorithm (ACO), and Particle Swarm Optimization (PSO) [24] are also evaluated for comparison. Table 2 lists the test

Table 1
NSCT-GWO-PCNN image denoising algorithm

Number	Functions	Range
F1	$f(x) = \sum_{i=1}^{n} x_i^2$	$[-100, 100]$
F2	$f(x) = \max\{\lvert x_i \rvert, 1 \le i \le n\}$	$[-100, 100]$
F3	$f(x) = \sum_{i=1}^{n} \frac{x_i^2}{4000} - \prod_{i=1}^{n} \cos(\frac{x_i}{\sqrt{i}}) + 1$	$[-600, 600]$
F4	$f(x) = \sum_{i=1}^{n} [x_i^2 - 10\cos(2\pi x_i) + 10]$	$[-5.12, 5.12]$

Figure 6
Benchmark function

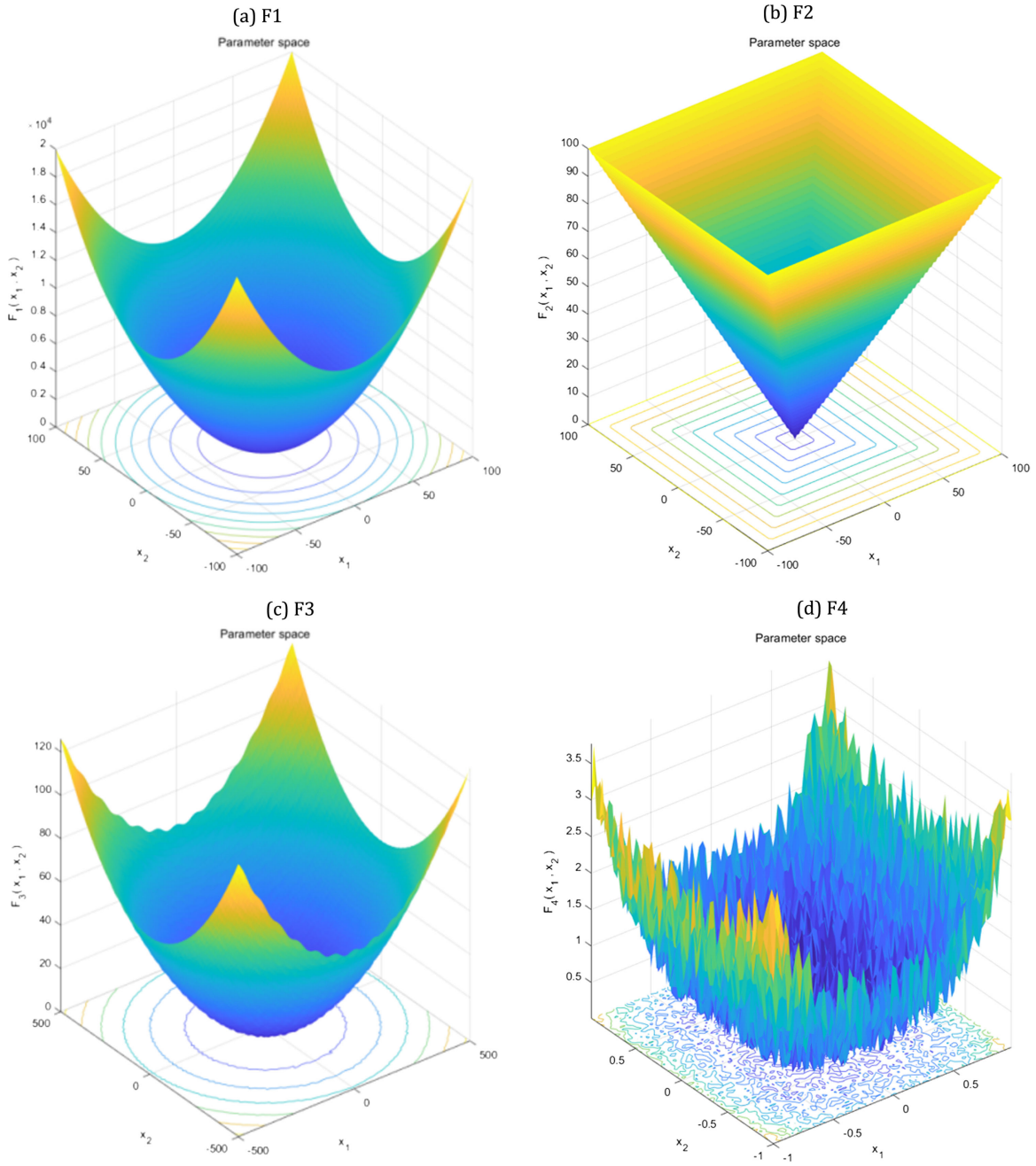

Table 2
Experimental results of comparison algorithms on four test functions

Number		GA	ACO	PSO	GWO
F1	Mean	3.45E-07	4.53E-07	5.85E-02	1.32E-08
	STD	2.82E-07	2.37E-07	3.65E-02	2.63E-08
F2	Mean	8.64E-05	3.41E-05	5.64E-03	2.42E-06
	STD	3.72E-05	6.78E-05	3.24E-03	1.58E-06
F3	Mean	358E-03	2.15E-11	4.58E-02	1.25E-12
	STD	8.76E-03	5.35E-11	8.87E-02	4.53E-12
F4	Mean	7.83E-03	9.87E-3	2.78E-02	7.86E-04
	STD	5.37E-03	2.35E-03	9.74E-02	7.27E-04

Figure 7
Convergence results of GWO, GA, ACO, and PSO

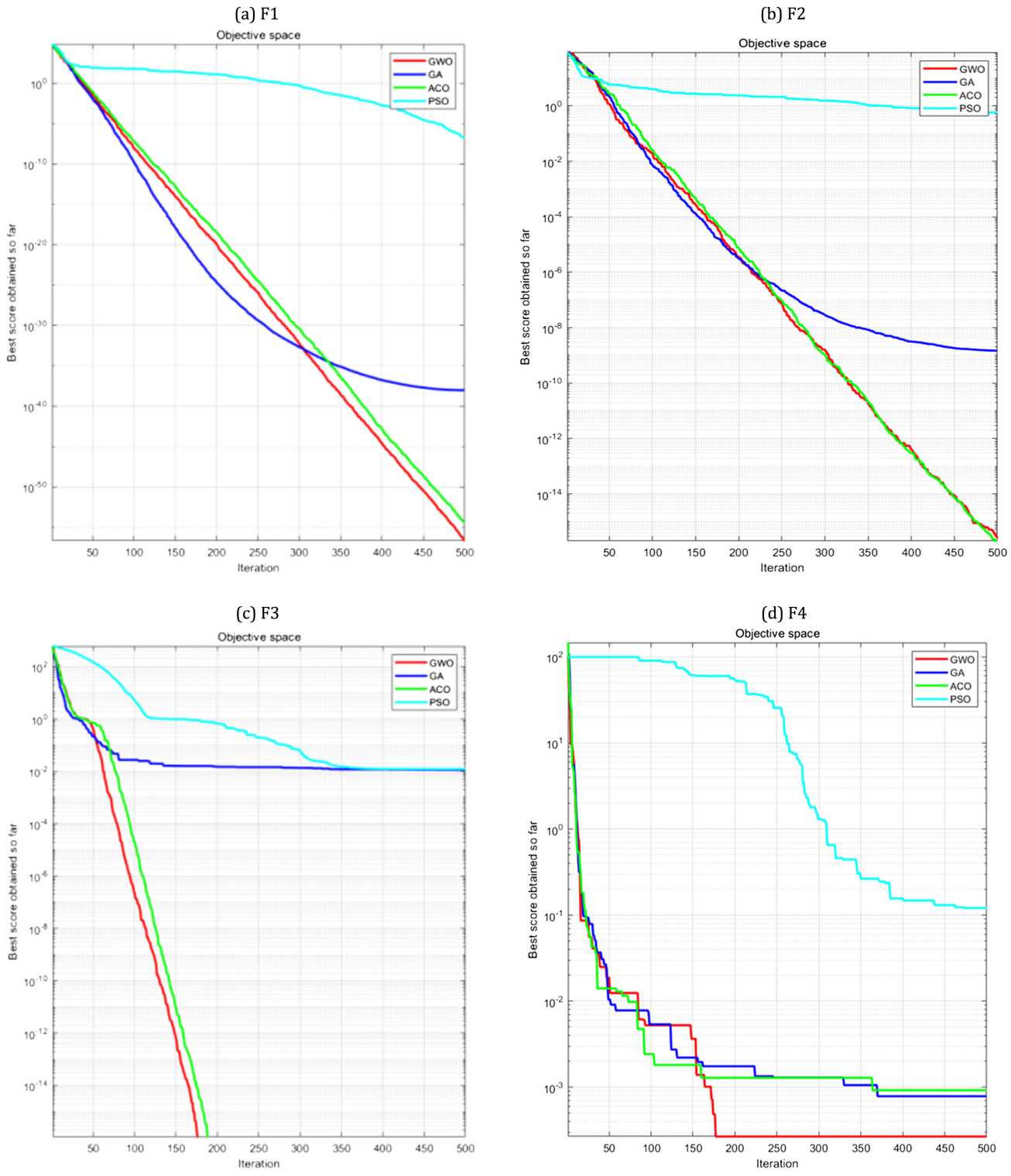

results of each algorithm on the benchmark function. The results reveal that GWO can converge faster than the PSO and ACO and can complete the global search optimization. GWO also obtains a better final solution than GA. At the same time, according to the numerical results, GWO obtained a higher solution accuracy, which indicates that the adaptive position updating strategy of individual GWO is a better improvement strategy.

Figure 7 shows the convergence curves of the four algorithms in four search spaces. The problems of premature convergence and early local fitness value cannot be ignored. For example, on F3, GA falls into local optimal solution at the 200th iteration, and it cannot jump out of local optimal solution until the end of algorithm iteration. As can be seen from the convergence diagram, GWO performs better than other algorithms. At the same

time, it can be observed from most of the curves that GWO has a good initial fitness value, indicating that the initialization strategy of the algorithm in this article has played an obvious role in enabling the algorithm to obtain the best fitness value.

4.2. Experimental denoising analysis

To further evaluate the NSCT-GWO-PCNN polarization image denoising optimization method proposed in this article, the objective function of the GWO was used to objectively evaluate the image performance parameters using an evaluation index, that is, the MSE. The degree of change in the image is measured by the normalized MSE (NMSE) of the image, which has a range of [0,1] after normalization and more clearly reveals the difference in parameters among the images. The MSE is calculated as follows:

$$MSE = \frac{1}{mn}\sum_{i=0}^{m-1}\sum_{j=0}^{n-1}[I(i,j) - K(i.j)]^2 \tag{17}$$

where $I(i,j)$ represents the gray value corresponding to the pixel points in row i and column j of the original polarization image; $K(i,j)$ represents the gray value corresponding to the pixel points in row i and column j of the denoised polarization image. For NMSE [25], higher values indicate that the denoising performance of the image is worse.

The SNR is the ratio of the power spectrum of the signal to the noise. A larger SNR indicates that the image contains less noise. SNR is calculated as follows:

$$SNR = 10\log_{10}\left[\frac{\sum_{i=0}^{m-1}\sum_{j=0}^{n-1} I(i,j)^2}{\sum_{i=0}^{m-1}\sum_{i=0}^{n-1}[(i,j) - K(i,j)]^2}\right] \tag{18}$$

The evaluation experiment in this study was run on a MATLAB2022, a platform equipped with an Intel® Core™ i7-7700 CPU, 16 GB of memory, and a 64-bit operating system.

The experimental data were captured by the self-made polarization camera. The polarization scene images include the details of buildings and cars. The actual collection of the polarized images is prone to noise interference. Moreover, the similarity between the polarization images and the image target is poor because of the precision of the polarization camera, lens dust, and the photographer's jitter. In addition, since the real image captured by polarization camera has no ground truth to provide for reference, it is often affected by uncertainties and imprecisions. Therefore, we fuzzy the polarized light image according to Versaci et al. [26], so as to improve the robustness of the method proposed. To enhance the levels of noise of the images in the experiment, we added salt-and-pepper noise to the original polarization image, because when imaging the polarized light sensor, there will be statistical fluctuations in some light quanta reaching the surface of the polarized array. We used additive salt-and-pepper noise in our enhanced noise experiments because polarization images are granular. The number of gray levels of the polarization image was set to 256, and the size of the image was increased to 244×204.

In this experiment, the GWO algorithm was used to optimize the inherent voltage constant V_T, decay time constant α_T, and neuron connection strength factor β_T of the PCNN model. The PCNN with adaptive parameters was used. The simulation is completed, which shows that the method has a certain feasibility. The parameters for the initial run of the PCNN model were manually set 0.5, 1, and 150, respectively.

After the PCNN completed the first image denoising, the GWO algorithm was used to adaptively seek the optimal solution. The process of seeking the optimal solution and the process of denoising were carried out simultaneously. First, the number of iterations of GWO algorithm was set to 100. The solution sets of PCNN parameters optimized by the GWO algorithm are listed in Table 3.

Table 3
GWO-optimized PCNN parameters

Number	β_T	V_T	α_T
1	0.7562	1.4475	258.4424
2	0.8563	1.0725	212.5581
3	0.9532	2.0127	233.4272
4	0.6994	2.1775	195.8413
5	0.8234	1.8645	196.4177
6	0.901	0.7753	173.8651
7	0.8427	1.9621	209.2786

In Table 3, the seven groups of solutions were optimized by the GWO algorithm. We selected one of them as the optimal parameters of PCNN for the polarization image denoising experiment.

Figures 8, 9, and 10 show the polarization images of three sets of scenes and the decomposed images under four polarization angles. The three sets of scenes all contain the polarization images of the scene and the target and also include the sky scene to complete the polarized light orientation experiment. It shows the scene polarization image with salt-and-pepper noise and the four decomposed polarization angle images. The experimental results after denoising and recombining the four polarization angle images using the NSCT-GWO-PCNN algorithm are shown in (f)–(i). It can be seen that the method proposed in this article restores the details of the scene polarization image completely. In the denoised polarization image, the edges of cars and buildings in the scene have been enhanced, and the contrast of the sky region has been enhanced by the neuron firing operation. In addition, in the enhanced noise experiment, the salt-and-pepper noise added to the original polarization image has also been removed. From the polarization image with noise, it can be seen that the polarization degree of the window is higher than the metal surface of the car. All the methods proposed in this article can restore the contour of the vehicle, and the overall polarization degree of the vehicle is basically the same and does not change with the change of the material. The method in this article keeps the trend of polarization degree while removing noise. The polarization information is recovered well and the average brightness is consistent.

In addition, to evaluate the advantages of the method in this article, we also used a traditional median filter (MF), residual neural network (ResNet), and the PCNN model with manually set parameters to conduct a comparative denoising experiment. The denoising performances of the four methods are shown in Figure 11. The MF is a classic method for removing salt-and-pepper noise in a polarization image. Because the polarization image contains an image synthesized from four polarization angle images, the MF can remove the noise to a certain extent from a polarization image with a single angle, but if the polarization images for all four angles are synthesized after denoising, the denoising effect is not satisfactory. To denoising an image using the traditional PCNN model, it is necessary to set the manual parameters many times, which may achieve a good denoising performance to a certain extent, but it does not fully leverage the denoising potential of the PCNN model, and it is too difficult to obtain parameters with good denoising performance. For ResNet, only the contour of the polarization image has been recovered well. The polarization degree of the whole car is basically the same and does not change with the change of material. However, there is a

Figure 8
NSCT-GWO-PCNN polarization image denoising results

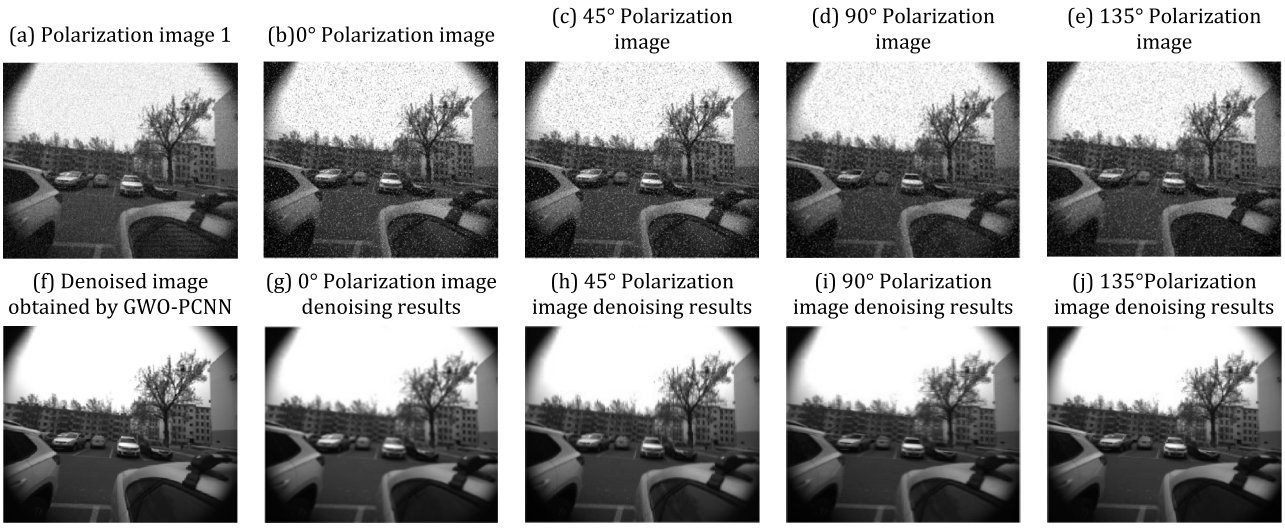

Figure 9
NSCT-GWO-PCNN polarization image denoising results

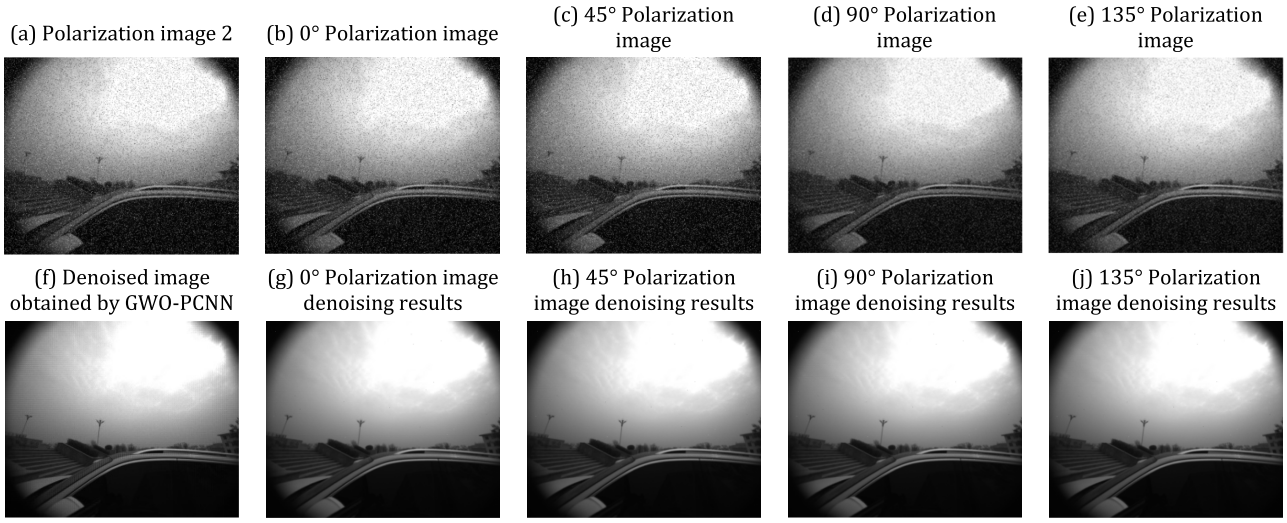

Figure 10
NSCT-GWO-PCNN polarization image denoising results

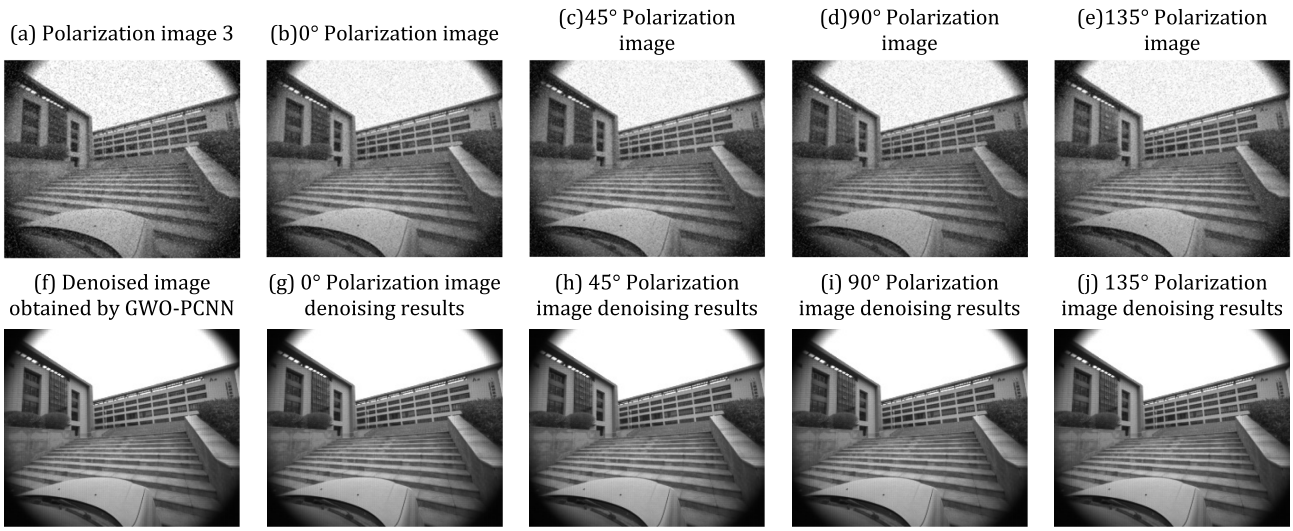

Figure 11
Denoising results with different methods

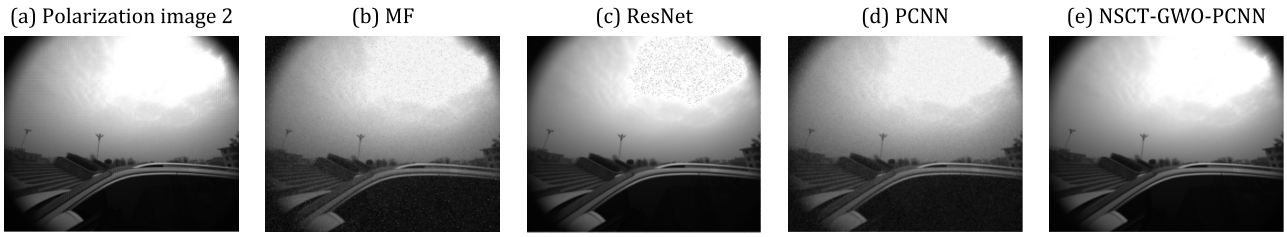

Table 4
Evaluation indices of various image denoising methods

	MF	PCNN	ResNet	NSCT-GWO-PCNN
NMSE	0.7522	0.9023	0.5682	0.4921
MSE	1.0347	1.7014	1.4387	1.3934
SNR	8.9051	9.1053	6.1272	7.6073

lot of noise in the important sky polarization information, which may be caused by the poor training effect. The PCNN method basically restores the contour of the image, but the details of the sky and the car in the polarization image are still slightly blurred, and the high polarization degree of the car roof is not well restored. In addition, the polarization image after MF processing appears very serious distortion. Although ResNet achieved good denoising effect, it has spent huge training costs and resources, and this process is tedious. Compared with these three methods, NSCT-GWO-PCNN has higher denoising efficiency.

Finally, to objectively evaluate the GWO-PCNN denoising algorithm, we computed the evaluation indicators in the objective function of the GWO, which can objectively evaluate the performance of image denoising and compare the GWO-PCNN with the MF. The parameters are compared with the polarization image denoised by the traditional PCNN model. Table 4 compares the evaluation indices (NMSE, MSE, and SNR) of the results of the polarization image in Figure 6. The results in the table show that the NMSE and MSE of the polarization image processed by the NSCT-GWO-PCNN algorithm are lower than those of the other algorithms, and the SNR is substantially improved. Therefore, it can be clearly seen from the experimental denoising result images and evaluation indices that the NSCT-GWO-PCNN denoising algorithm effectively suppresses image noise.

5. Conclusion

In this article, an improved PCNN polarization image denoising method based on GWO and NSCT was proposed. Polarization images were devised using the NSCT, and the PCNN parameters were optimized by adaptive GWO, and denoising experiments were carried out on decomposed polarization channel images. Compared with three methods, the proposed method maintains the edge and details of the image better, effectively removes the salt-and-pepper noise added to enhance the levels of noise, and performs better than three methods with respect to the objective image evaluation indices.

Funding Support

This work was supported in part by the National Natural Sciences Foundation of China (61973281, 51821003, 51922009), Foundation of Science and Technology on Electro-Optical Information Security control Laboratory (2021JCJQLB055010), Key research and development project of Shanxi Province (202003D111003), Excellent Youngth foundation of Shanxi Province (202103021222011), Aviation Science Foundation (2018ZCU0002), Shanxi Province Key Laboratory of Quantum Sensing and Precision Measurement (201905D121001), 1331 Project of Shanxi Province.

Ethical Statement

This study does not contain any studies with human or animal subjects performed by any of the authors.

Conflicts of Interest

The authors declare that they have no conflicts of interest to this work.

Data Availability Statement

Data sharing is not applicable to this article as no new data were created or analyzed in this study.

References

[1] Liu, J., & Chen, X. (2021). Temperature drift compensation of a FOG based on an HKSVM optimized by an improved hybrid BAS-GSA algorithm. *Applied Optics*, *60*(34), 10539–10547. https://doi.org/10.1364/AO.440887

[2] Lindblad, T., & Kinser, J. M. (2005). *Image processing using pulse-coupled neural networks*. Germany: Springer.

[3] Shi, M., Fan, X., & Zhang, J. (2001). On auto-wave travelling of discrete pulse-coupled neural networks. In *International Conference on Neural Information Processing*.

[4] Li, G., Li, H., & Wu, T. (2005). The image enhancement based on modified pulse coupled neural network and genetic algorithm. *Journal of Test and Measurement Technology*, *19*(3), 304.

[5] Fang, Y., Qi, F. H., & Pei, B. Z. (2005). PCNN implementation and applications in image processing. *Journal of Infrared and Millimeter Waves*, *24*(4), 291–295.

[6] Guo, S., Cheng, C., Pu, G., & Deng, S. (2009). A novel algorithm for remote image progressive coding based on ROI. In *2009 IEEE International Conference on Automation and Logistics*, 860–864. https://doi.org/10.1109/ICAL.2009.5262801

[7] Wang, Z., Xu, M., & Zhang, Y. (2022). Quantum pulse coupled neural network. *Neural Networks*, *152*, 105–117. https://doi.org/10.1016/j.neunet.2022.04.007

[8] Gilboa, E., Cunningham, J. P., Nehorai, A., & Gruev, V. (2014). Image interpolation and denoising for division of focal plane sensors using Gaussian processes. *Optics Express*, *22*(12), 15277–15291. https://doi.org/10.1364/OE.22.015277

[9] Zhang, J., Luo, H., Liang, R., Zhou, W., Hui, B., & Chang, Z. (2017). PCA-based denoising method for division of focal plane polarimeters. *Optics Express*, *25*(3), 2391–2400. https://doi.org/10.1364/OE.25.002391

[10] Deng, X., Yan, C., & Ma, Y. (2020). PCNN mechanism and its parameter settings. *IEEE Transactions on Neural Networks and Learning Systems*, *31*(2), 488–501. https://doi.org/10.1109/TNNLS.2019.2905113

[11] Sang, Y., Lv, J., Qu, H., & Yi, Z. (2016). Shortest path computation using pulse-coupled neural networks with restricted autowave. *Knowledge-Based Systems*, *114*, 1–11. https://doi.org/10.1016/j.knosys.2016.08.027

[12] Gu, X., Guo, S., & Yu, D. (2002). A new approach for noise reducing of image based on PCNN. *Journal of Electronics & Information Technology*, *24*(10), 1304–1309.

[13] Zhao, D., Liu, Y., Wu, X., Dong, H., Wang, C., Tang, J., . . . , & Liu, J. (2022). Attitude-induced error modeling and compensation with GRU networks for the polarization compass during UAV orientation. *Measurement*, *190*. https://doi.org/10.1016/j.measurement.2022.110734

[14] Wang, Z., Ma, Y., Cheng, F., & Yang, L. (2010). Review of pulse-coupled neural networks. *Image and Vision Computing*, *28*(1), 5–13. https://doi.org/10.1016/j.imavis.2009.06.007

[15] Wang, X. Y., Yang, H. Y., Zhang, Y., & Fu, Z. K. (2013). Image denoising using SVM classification in nonsubsampled contourlet transform domain. *Information Sciences*, *246*, 155–176. https://doi.org/10.1016/j.ins.2013.05.028

[16] Zhang, Q., & Guo, B. L. (2009). Multifocus image fusion using the nonsubsampled contourlet transform. *Signal Processing*, *89*(7), 1334–1346. https://doi.org/10.1016/j.sigpro.2009.01.012

[17] Gupta, E., & Saxena, A. (2015). Robust generation control strategy based on grey wolf optimizer. *Journal of Electrical Systems*, *11*(2), 174–188.

[18] Mirjalili, S., Mirjalili, S. M., & Lewis, A. (2014). Grey wolf optimizer. *Advances in Engineering Software*, *69*, 46–61. https://doi.org/10.1016/j.advengsoft.2013.12.007

[19] Lu, C., Gao, L., & Yi, J. (2018). Grey wolf optimizer with cellular topological structure. *Expert Systems with Applications*, *107*, 89–114. https://doi.org/10.1016/j.eswa.2018.04.012

[20] Zhu, Y., Jiang, W., Kong, X., Quan, L., & Zhang, Y. (2017). A chaos wolf optimization algorithm with self-adaptive variable step-size. *AIP Advances*, *7*(10), 105024. https://doi.org/10.1063/1.5005130

[21] Banu, S. S., & Baskaran, K. (2018). Hybrid FGWO based FLCs modeling for performance enhancement in wireless body area networks. *Wireless Personal Communications*, *100*(3), 1163–1199. https://doi.org/10.1007/s11277-018-5626-4

[22] Cheng, Y., Tian, L., Yin, C., Huang, X., Cao, J., & Bai, L. (2018). Research on crack detection applications of improved PCNN algorithm in MOI nondestructive test method. *Neurocomputing*, *277*, 249–259. https://doi.org/10.1016/j.neucom.2017.02.099

[23] Miller, B., & Ziemiański, L. (2020). Optimization of dynamic behavior of thin-walled laminated cylindrical shells by genetic algorithms and deep neural networks supported by modal shape identification. *Advances in Engineering Software*, *147*, 102830. https://doi.org/10.1016/j.advengsoft.2020.102830

[24] Shen, C., Wang, D., Tang, S., Cao, H., & Liu, J. (2017). Hybrid image noise reduction algorithm based on genetic ant colony and PCNN. *The Visual Computer*, *33*(11), 1373–1384. https://doi.org/10.1007/s00371-016-1325-x

[25] Chen, Y., Park, S. K., Ma, Y., & Ala, R. (2011). A new automatic parameter setting method of a simplified PCNN for image segmentation. *IEEE Transactions on Neural Networks*, *22*(6), 880–892. https://doi.org/10.1109/TNN.2011.2128880

[26] Versaci, M., Angiulli, G., Crucitti, P., de Carlo, D., Laganà, F., Pellicanò, D., & Palumbo, A. (2022). A fuzzy similarity-based approach to classify numerically simulated and experimentally detected carbon fiber-reinforced polymer plate defects. *Sensors*, *22*(11), 4232. https://doi.org/10.3390/s22114232

How to Cite: Li, Y., Sun, Y., & Feng, K. (2024). Improved PCNN Polarization Image Denoising Method Based on Grey Wolf Algorithm and Non-Subsampled Contourlet Transform. *Journal of Computational and Cognitive Engineering*. https://doi.org/10.47852/bonviewJCCE3202943